Materials Letters 245 (2019) 192–195

Contents lists available at ScienceDirect

Materials Letters

journal homepage: www.elsevier.com/locate/mlblue

Nitrogen-doped reduced graphene oxide as excellent electrode materials for high performance energy storage device applications

Rajneesh Kumar Mishra [a], Gyu Jin Choi [a], Youngku Sohn [b], Seung Hee Lee [c,*], Jin Seog Gwag [a,*]

[a] Department of Physics, Yeungnam University, Gyeongsan, Gyeongbuk 38541, South Korea
[b] Department of Chemistry, Chungnam National University, Daejeon, South Korea
[c] Applied Materials Institute for BIN Convergence, Department of BIN Convergence Technology and Department of Polymer-Nano Science and Technology, Chonbuk National University, Jeonju, Jeonbuk 561-756, South Korea

ARTICLE INFO

Article history:
Received 24 January 2019
Received in revised form 4 March 2019
Accepted 5 March 2019
Available online 6 March 2019

Keywords:
N-doped RGO
High specific capacity
High energy density
Voltage holding test
Leakage current
Self-discharge mechanisms

ABSTRACT

Herein, we studied the nitrogen-doped reduced graphene oxide (N-doped RGO) as an excellent electrode materials in energy storage applications. The N-doped RGO based solid-state symmetric supercapacitor (SSC) device shows high specific capacity (141.1 mA h g^{-1}) and high energy density (28.2 W h kg^{-1}). The N-doped RGO based SSC device illustrates the notable stabilities of ~95.4% via 10,000 galvanostatic charging-discharging (GCD) cycles and ~93.2% via 8 h voltage holding tests. Additionally, the N-doped RGO based SSC device shows outstanding self-discharge properties, which retains the voltages of 0.65 V, 0.69 V, 0.68 V and 0.70 V of its initial voltage (1.2 V) after each GCD cycling + 2 h voltage holding test + 2 h self-discharge test, respectively, which vindicates the excellent state of health of the supercapacitor device.

1. Introduction

Modern civilization is enfolded by the endless handy gadgets, especially mobile phones as communication devices, sensors and artificial intelligence (AI) as public safety & security, and health conscious wearable fitness tools [1,2]. However, these all handy gadgets/security devices require clean, affordable, durable, and fast chargeable energy storage systems. Recently, electrochemical capacitors have attracted considerable attention due to their inherent properties such as high power density, fast charging and highly durable [3,4] and have commenced in hybrid vehicles, electronics toys and portable devices, including memory backup systems [5,6]. Therefore, the large scale production of supercapacitors would be a next step towards substituting batteries, however, the lower energy density, percolation of electrolytes, and less investigations to voltage holding test, leakage current and self-discharge characteristics make them difficult to take forward. On the other hand, the nanostructured materials are the backbone in electrode preparation, which plays a significant role in boosting the electrochemical properties of the supercapacitor device [7]. Therefore, two-dimensional (2D) layered materials, polymer based solid-state electrodes, and voltage holding and self-discharge tests are the key parameters, which can be optimized to deal with the current scenario faced by the supercapacitors.

Reduced graphene oxide (RGO) is an outstanding 2D nanomaterials of the carbon family with sp^2 hybridized carbon atoms, enriched with high surface area and inherent electrical and mechanical properties makes it ubiquitous in several applications such as gas sensors, batteries, supercapacitors and FETs [8,9]. However, the addition of heteroatoms (N, B or F) on the surface or in the bulk of RGO can provide an effective approach to enhance the pair of electrons in the host system, which harmonize the electron donor-acceptor behaviour [10], and therefore, can improve the electrochemical properties of supercapacitor device.

In this letter, we fabricated the nitrogen-doped reduced graphene oxide (N-doped RGO) based symmetric supercapacitor device for energy storage applications. The SSC device exhibits large voltage window of 1.2 V and high specific capacity. The SSC device depicts the outstanding stability via galvanostatic charging-discharging (GCD) cycles and voltage holding test, which results small leakage current. The self-discharge characteristics describes the good health of supercapacitor device and further provides deeper insight to understand the mechanisms of diffusion-controlled processes or leakage current through internal resistance.

* Corresponding authors.
E-mail addresses: lsh1@jbnu.ac.kr (S.H. Lee), sweat3000@ynu.ac.kr (J.S. Gwag).

https://doi.org/10.1016/j.matlet.2019.03.010
0167-577X/

2. Experimental details

Graphene oxide (GO) was synthesized from natural graphite (Alfa Aesar) using the modified Hummers method [11]. The prepared GO (30 mg) solution in 60 ml de-ionized (DI) water with ultrasonication, and then urea (900 mg) was added slowly as nitrogen (N) dopant and kept stirring for 30 min. Further, the prepared solution was transferred into a Teflon-lined autoclave of 100 ml capacity and kept it under the convection oven at 160 °C for 12 h. The synthesized precipitate was centrifuged, washed with

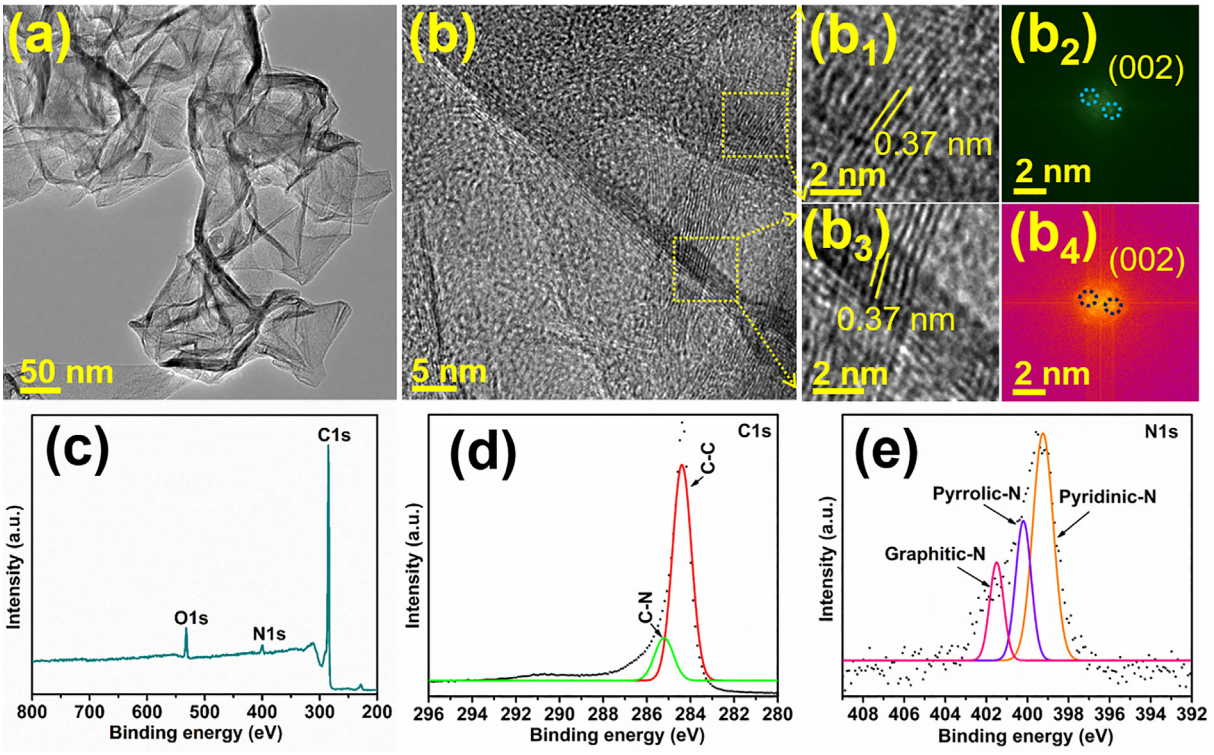

Fig. 1. (a) TEM image, (b) HRTEM image, (b_1, b_3) enlarged area of HRTEM image and (b_2, b_4) their corresponding FFT analyses, (c) XPS survey spectrum, (d) fitting of narrow scan XPS peaks of C1s and (e) fitting of narrow scan XPS N1s peaks of N-doped RGO.

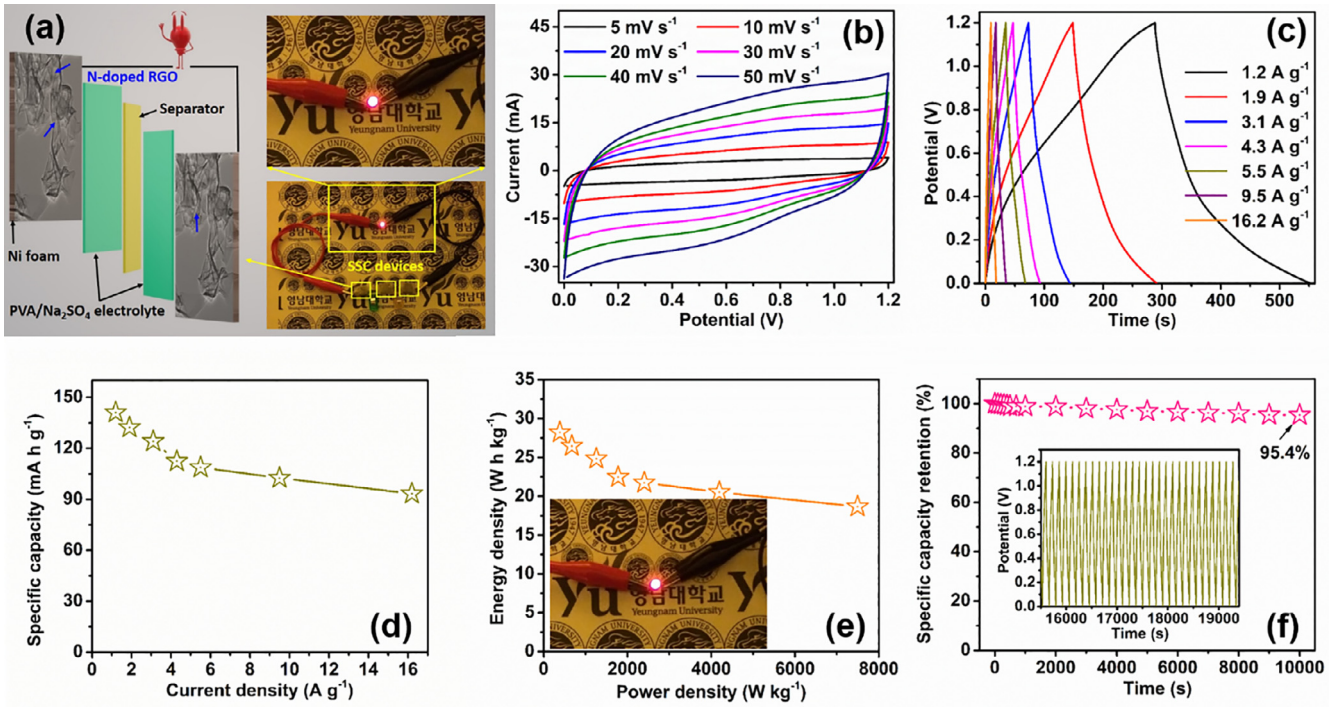

Fig. 2. (a) Schematic representation of the N-doped RGO based SSC device and demonstration of red LED, (b) CV plots, (c) GCD profiles, (d) specific capacity, (e) energy density and (f) Stability via GCD cycles at 3.1 A g^{-1}.

DI water and ethanol for several times, and dried at 80 °C in vacuum to obtain nitrogen-doped reduced graphene oxide (N-doped RGO). The material characterization techniques, electrode preparation and solid-state symmetric supercapacitor (SSC) device fabrication are discussed in the supporting information.

3. Results and discussion

Fig. 1(a) shows the transmission electron microscopy (TEM) image of N-doped RGO layers, which are folded, twisted, crumbled and overlapped, can be beneficial in supercapacitor applications. Fig. 1(b, b_1 and b_3) depicts the high resolution TEM (HRTEM) images of N-doped RGO with overlapped and crossed lattice fringes of 0.37 nm. Fig. 1(b_2, b_4) shows the fast Fourier transform (FFT) images of N-doped RGO with (0 0 2) lattice plane. Fig. 1(c-e) indicates the x-ray photoelectron spectroscopy (XPS) survey and narrow spectra of N-doped RGO with C1s (284.3 eV), O1s and N1s (399.37) peaks, respectively [11]. In addition, the fitting of narrow scan spectra of C1s and N1s in Fig. 1(d, e), confirm the presence of C-N, C-C, graphitic-N, pyrrolic-N and pyridinic-N peaks of the nitrogen-doped functional groups in the RGO system, which also play a key role in pseudocapacitance behaviour of electrochemical capacitors [12]. Furthermore, the Raman and Fourier-transform infrared (FTIR) spectroscopy results also studied and discussed in the supporting information [Fig. S1(a, b)], which confirms the successful synthesis of N-doped RGO and justifies the TEM and XPS results.

Fig. 2(a) shows the schematic representation of exploded view of N-doped RGO based SSC device, which displays the illumination of a red light emitting diode (LED). Fig. 2(b) shows the CV plots of N-doped RGO based SSC device at different scan rates (5 mV s^{-1} to 50 mV s^{-1}). This exhibits the capacitive as well as pseudocapacitive nature, which is further justified by the charge storage kinetics mechanism as discussed in the Fig. S2(a, b) (evaluated by using Eq. S1) [12]. The nitrogen-doped functional groups that bond to the RGO structure can be considered as pyridinic-N, pyrrolic-N, quaternary-N, and pyridinic-N-oxide types, are supposed to deliver pseudocapacitance through the redox reactions between N-doped structures and protons. Here, pyridinic-N and pyrrolic-N structures are playing a key role in contributing pseudocapacitance properties of N-doped RGO based SSC device [12]. From Fig. 2(c), the linear portion in the GCD plots contributes EDLC whereas plateau region indicates the small contribution of pseudocapacitance, which plays a key role in determining the specific capacity of supercapacitor via reversible adsorption-desorption of electrolyte gel ions and redox reactions [12,13]. Fig. 2(d) shows the high specific capacity (evaluated by using Eq. S2) of 141.1 mA h g^{-1} at a current density of

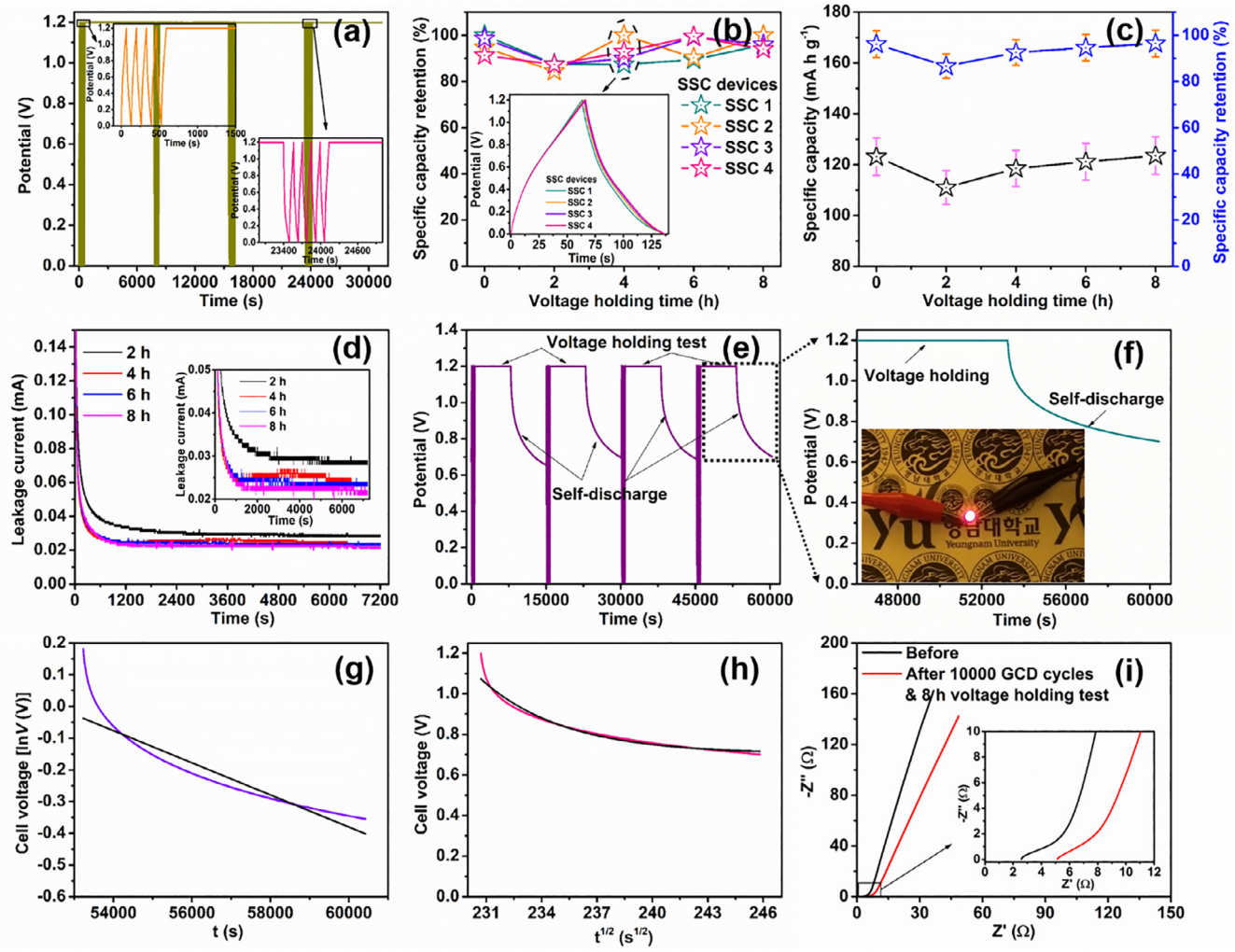

Fig. 3. N-doped RGO based SSC device; (a) Voltage holding test (inset: enlarged portion of GCD cycles), (b) reproducibility via voltage holding test (inset: GCD cycles of four SSC devices after 4 h voltage holding test), (c) specific capacity and retention at 3.1 A g^{-1}, (d) leakage current, (e) GCD cycles + voltage holding + self-discharge characteristics, (f) voltage holding + self-discharge characteristics, fitting curves of self-discharge models (g) leakage current through internal resistance (Eq. S5) and (h) diffusion-controlled processes (Eq. S6), and (i) EIS spectra before/ after 10,000 GCD cycles and 8 h voltage holding test.

1.2 A g^{-1} and 93.4 mA h g^{-1} at a current density of 16.2 A g^{-1}, respectively. Fig. 2(e) illustrates high energy and power densities (evaluated by using Eqs. S3 & S4) of 28.2 W h kg^{-1} and 7494.7 W kg^{-1}, respectively. Fig. 2(f) elucidates the excellent GCD cycling stability of 95.4% (inset shows the in-between GCD cycles).

Fig. 3(a) shows the GCD cycling + voltage holding tests of SSC device for 8 h (inset shows the GCD cycles in between voltage holding test), which results good voltage capabilities of SSC device. Fig. 3(b) shows the reproducibility via voltage holding tests (inset depicts the GCD cycles of four SSC devices), which reveals admirable reproducibility of SSC device. Fig. 3(c) displays the average specific capacity and average specific capacity retention evaluated by the four SSC devices, which offers the outstanding stability of 93.2% after 8 h voltage holding tests. Fig. 3(d) shows the small leakage currents of 0.028 mA, 0.024 mA, 0.023 mA and 0.021 mA during 2 h, 4 h, 6 h and 8 h voltage holding tests, which suggests that there is no internal resistance formed during voltage holding test. Fig. 3(e) shows GCD cycles + 2 h voltage holding test + 2 h self-discharge plots of the SSC device for 16 h and displays good voltage holding capabilities of 0.65 V, 0.69 V, 0.68 V and 0.70 V of its initial voltage (1.2 V) after GCD cycles + 2 h voltage holding test + 2 h self-discharge test, respectively. Thus, these self-discharge results validate the stability results obtained from GCD cycles [Fig. 2(f)] and voltage holding tests [Fig. 3(a–c)] and also the results of leakage current [Fig. 3(d)]. Fig. 3(f) reveals the enlarged portion of self-discharge plot [Fig. 3(e)] to further study the self-discharge mechanisms of the SSC device. To understand the self-discharge mechanisms, two models such as leakage current over internal resistance (Eq. S5) and the diffusion controlled processes (Eq. S6) were used to investigate the SSC device's performance credibility.

Fig. 3(g) shows the ln V vs t plot of self-discharge by applying the Eq. S5. The self-discharge results deviates from linear nature, which shows that the self-discharge characteristics of SSC device is not due to leakage current. Fig. 3(h) shows the V vs $t^{1/2}$ plot via using Eq. S6. This shows that the Eq. S6 fitted well with the self-discharge results and therefore, it demonstrates that the diffusion controlled process plays a significant role over leakage current. Fig. 3(i) elucidates the electrochemical impedance spectra (EIS) of the SSC device before/ after 10,000 GCD cycles and 8 h voltage holding tests. From the equivalent circuit model, the values of internal resistance (R_s) are 2.6 Ω/5.2 Ω, interfacial charge transfer resistance (R_{ct}) are 1.7 Ω/1.9 Ω and the Warburg impedance (W_z) are 5.3 Ω/3.6 Ω before/after 10,000 GCD cycles & 8 h voltage holding test, respectively. The Bode plots [see Fig. S3] and Randles plots [See Fig. S4] (fitted by using Eq. S7) were studied and discussed in the supporting information.

4. Conclusions

In conclusion, the N-doped RGO based SSC device shows outstanding electrochemical behaviour. This demonstrates excellent stability via GCD cycles and voltage holding tests. The self-discharge results vindicates stability results investigated by the GCD cycles and voltage holding test. Furthermore, SSC device shows the high specific capacity, high energy density and low leakage current. Therefore, the N-doped RGO can be an excellent electrode material for energy storage device applications.

Declaration of interests

There are no conflicts to declare.

Acknowledgements

This work was supported through the Basic Science Research Program through the National Research foundation of Korea (NRF) funded by the Ministry of Science, ICT, and Future Planning (Grant No. 2016R1D1A3B03932396).

Appendix A. Supplementary data

Supplementary data to this article can be found online at https://doi.org/10.1016/j.matlet.2019.03.010.

References

[1] P. Sun, W. He, H. Yang, R. Cao, J. Yin, C. Wang, X. Xu, Nanoscale 10 (2018) 19004–19013.
[2] K.S. Kumar, N. Choudhary, Y. Jung, J. Thomas, ACS Energy Lett. 3 (2018) 482–495.
[3] (a) T. An, W. Cheng, J. Mater. Chem. A 6 (2018) 15478–15494;
(b) Y. Han, Q. Zhang, N. Hu, X. Zhang, Y. Mai, J. Liu, X. Hua, H. Wei, Chin. Chem. Lett. 28 (2017) 2269–2273.
[4] (a) Q. Shan, X. Mu, M. Alhabeb, C.E. Shuck, D. Pang, X. Zhao, X.-F. Chu, Y. Wei, F. Du, G. Chen, Y. Gogotsi, Y. Gao, Y. Dall'Agnese, Electrochem. Commun. 96 (2018) 103–107;
(b) X. Zhang, L. Yao, S. Liu, Q. Zhang, Y. Mai, N. Hu, H. Wei, Mater. Today Energy 7 (2018) 141–148.
[5] G.S.R. Raju, E. Pavitra, G. Nagaraju, S.C. Sekhar, S.M. Ghoreishian, C.H. Kwak, J.S. Yu, Y.S. Huh, Y.-K. Han, J. Mater. Chem. A 6 (2018) 13178–13190.
[6] (a) S. Zhu, P.-L. Taberna, N. Zhao, P. Simon, Electrochem. Commun. 96 (2018) 6–10;
(b) Y. Han, N. Hu, S. Liu, Z. Hou, J. Liu, X. Hua, Z. Yang, L. Wei, L. Wang, H. Wei, Nanotechnology 28 (2017) 33LT01.
[7] R.K. Mishra, M. Krishnaih, S.Y. Kim, A.K. Kushwaha, S.H. Jin, Mater. Lett. 236 (2019) 167–170.
[8] T.X. Tran, H. Choi, C.H. Che, J.H. Sul, I.G. Kim, S.-M. Lee, J.-H. Kim, J.B. In, ACS Appl. Mater. Interfaces 10 (2018) 39777–39784.
[9] Y. Shi, D. Yang, R. Yu, Y. Liu, J. Qu, B. Liu, Z.-Z. Yu, ACS Appl. Energy Mater. 1 (2018) 4186–4195.
[10] J. Zhao, H. Lai, Z. Lyu, Y. Jiang, K. Xie, X. Wang, Q. Wu, L. Yang, Z. Jin, Y. Ma, J. Liu, Z. Hu, Adv. Mater. 27 (2015) 3541–3545.
[11] X.-Y. Pei, D.-C. Mo, S.-S. Lyu, J.-H. Zhang, Y.-X. Fu, Appl. Surf. Sci. 465 (2019) 470–477.
[12] (a) R.K. Mishra, J.H. Ryu, H. In Kwon, S.H. Jin, J. Mater. Chem. A 6 (2018) 15253–15264;
(b) S.M. Li, S.-Y. Yang, Y.-S. Wang, H.-P. Tsai, H.-W. Tien, S.-T. Hsiao, W.-H. Liao, C.-L. Chang, C.-C.M. Ma, C.-C. Hu, J. Power Sources 278 (2015) 218–229.
[13] J. Wang, T. Park, J.W. Yi, B. Ding, J. Henzie, Z. Chang, H. Dou, X. Zhang, Y. Yamauchi, Nanoscale Horiz. 4 (2019) 526–530.